

## Supplemental material

Fan et al., <https://doi.org/10.1084/jem.20181442>

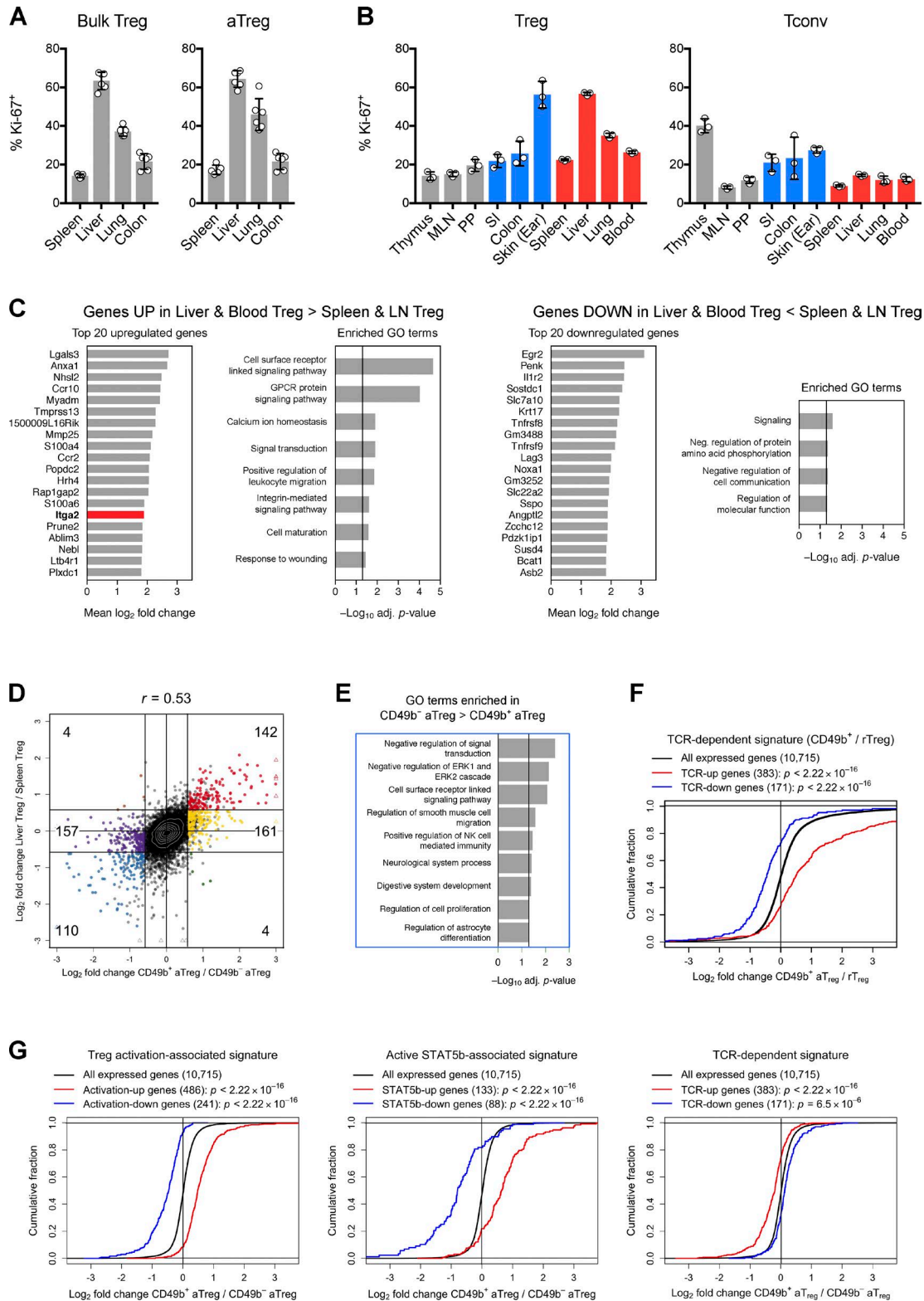
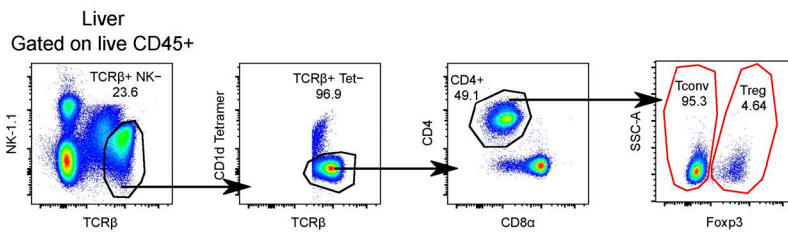
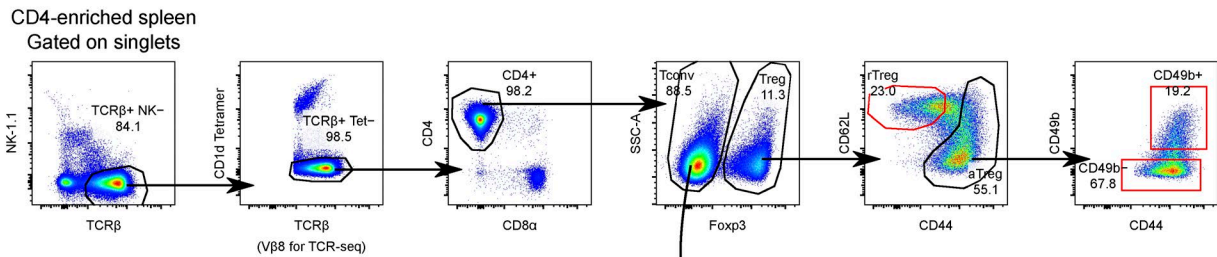


Figure S1. **Flow cytometric and RNA-seq analysis of hepatic and splenic Treg cells.** Related to Fig. 1 and Fig. 2. **(A)** Percentage of Ki-67<sup>+</sup> cells among bulk Treg or CD44<sup>hi</sup> aTreg cells in tissues of B6 mice. **(B)** Percentage of Ki-67<sup>+</sup> cells among CD4<sup>+</sup> Foxp3<sup>+</sup> (Treg) cells or CD4<sup>+</sup> Foxp3<sup>-</sup> (Tconv) cells in tissues of B6 mice. **(C)** Top 20 genes and enriched GO terms up- or down-regulated in liver and blood Treg cells compared with spleen and portal LN Treg cells. **(D)** Log<sub>2</sub> FC in gene expression between splenic CD49b<sup>+</sup> and CD49b<sup>-</sup> aTreg cells plotted against log<sub>2</sub> FC between liver and spleen Treg cells. **(E)** GO terms enriched among genes down-regulated in CD49b<sup>+</sup> versus CD49b<sup>-</sup> aTreg cells. **(F)** Cumulative distribution of CD49b<sup>+</sup>/rTreg cell log<sub>2</sub> FCs, of the Treg genes up- or down-regulated in a TCR-dependent manner (Levine et al., 2017). **(G)** Cumulative distribution of CD49b<sup>+</sup>/CD49b<sup>-</sup> aTreg log<sub>2</sub> FCs of the Treg cell genes up- or down-regulated with activation in an inflammatory environment (left; Arvey et al., 2014); through expression of an active form of STAT5b (center; Chinen et al., 2016); or in a TCR-dependent manner (right; Levine et al., 2017).

**A** RNA-seq of liver, spleen, blood, portal LN Treg and Tconv



**B** RNA-seq and TCR-seq of spleen Treg and Tconv subsets



**C** Single-cell sequencing of spleen Treg and Tconv



Figure S2. **Gating strategies for cell sorting and flow cytometry.** (A) Gating strategy for RNA-seq of bulk tissue Treg and Tconv cells. (B) Gating strategy for RNA-seq and TCR-seq of splenic Treg and Tconv cell subsets defined by activation markers. This gating strategy was also used for flow cytometric analyses of Treg cell subsets in lymphoid and NLTs. (C) Gating strategy for scRNA-seq of splenic Treg and Tconv cells.

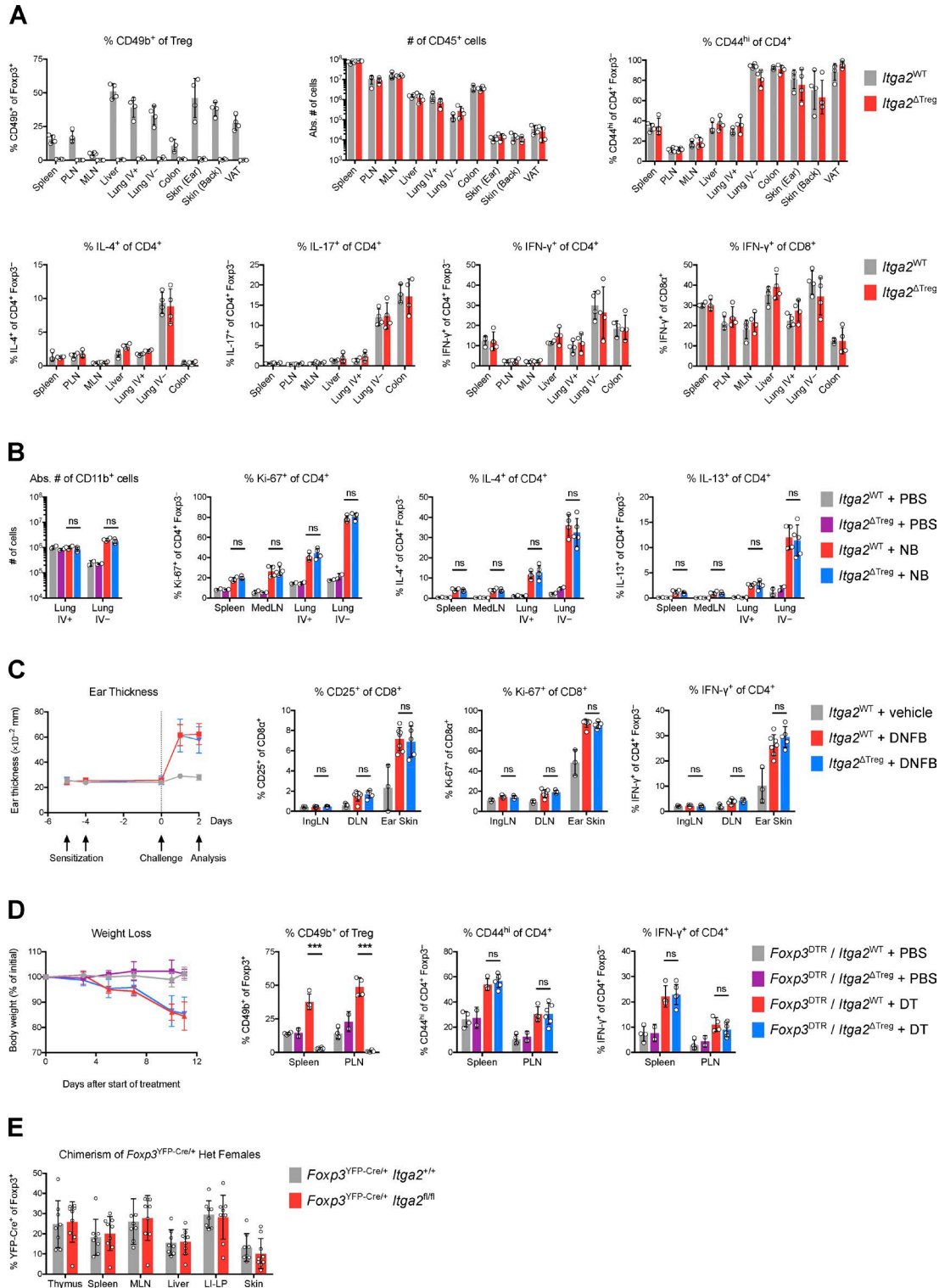


Figure S3. **Expression of CD49b in Treg cells is dispensable for maintenance of immune homeostasis.** Related to Fig. 3. **(A)** Percentage of CD49b<sup>+</sup> Treg cells; absolute number of CD45<sup>+</sup> cells; percentage of activated (CD44<sup>hi</sup>) Tconv cells; or IL-4, IL-17, and IFN-γ production by CD4<sup>+</sup> or CD8<sup>+</sup> T cells in 8-wk-old *Itga2*<sup>WT</sup> (*Foxp3*<sup>YFP-Cre</sup> *Itga2*<sup>+/+</sup>) or *Itga2*<sup>ΔTreg</sup> (*Foxp3*<sup>YFP-Cre</sup> *Itga2*<sup>fl/fl</sup>) mice. **(B)** *Itga2*<sup>WT</sup> or *Itga2*<sup>ΔTreg</sup> mice were infected with *N. brasiliensis* (NB). After 7 d, the absolute number of CD11b<sup>+</sup> cells and the percentages of Ki-67<sup>+</sup>, IL-4<sup>+</sup>, or IL-13<sup>+</sup> Tconv cells are shown. IV+, intravascular; IV-, extravascular. **(C)** *Itga2*<sup>WT</sup> or *Itga2*<sup>ΔTreg</sup> mice were sensitized and then challenged with dinitrofluorobenzene (DNFB). Ear thickness, CD25 and Ki-67 expression by CD8<sup>+</sup> T cells, and IFN-γ production by CD4<sup>+</sup> T cells were measured. IngLN, inguinal LN. DLN, (ear) draining LN. **(D)** Chimeras of 90% *Foxp3*<sup>ΔTreg</sup> and 10% *Itga2*<sup>WT</sup> or *Itga2*<sup>ΔTreg</sup> bone marrow were given DT. Weight loss, percentage of CD49b<sup>+</sup> Treg cells, percentage of activated Tconv cells, and IFN-γ production by Tconv cells are shown. **(E)** Treg cell chimerism in various tissues of 3–4-mo-old heterozygous female *Foxp3*<sup>YFP-Cre/+</sup> *Itga2*<sup>+/+</sup> or *Itga2*<sup>fl/fl</sup> mice. Cytokine restimulation was done using PMA/ionomycin in A, C, and D, and α-CD3/α-CD28 antibodies in B. Data in A–D are representative of two to four independent experiments each. Data in E are pooled from two independent experiments (n = 8–9 per group). \*\*\*, P ≤ 0.001 by paired t test.

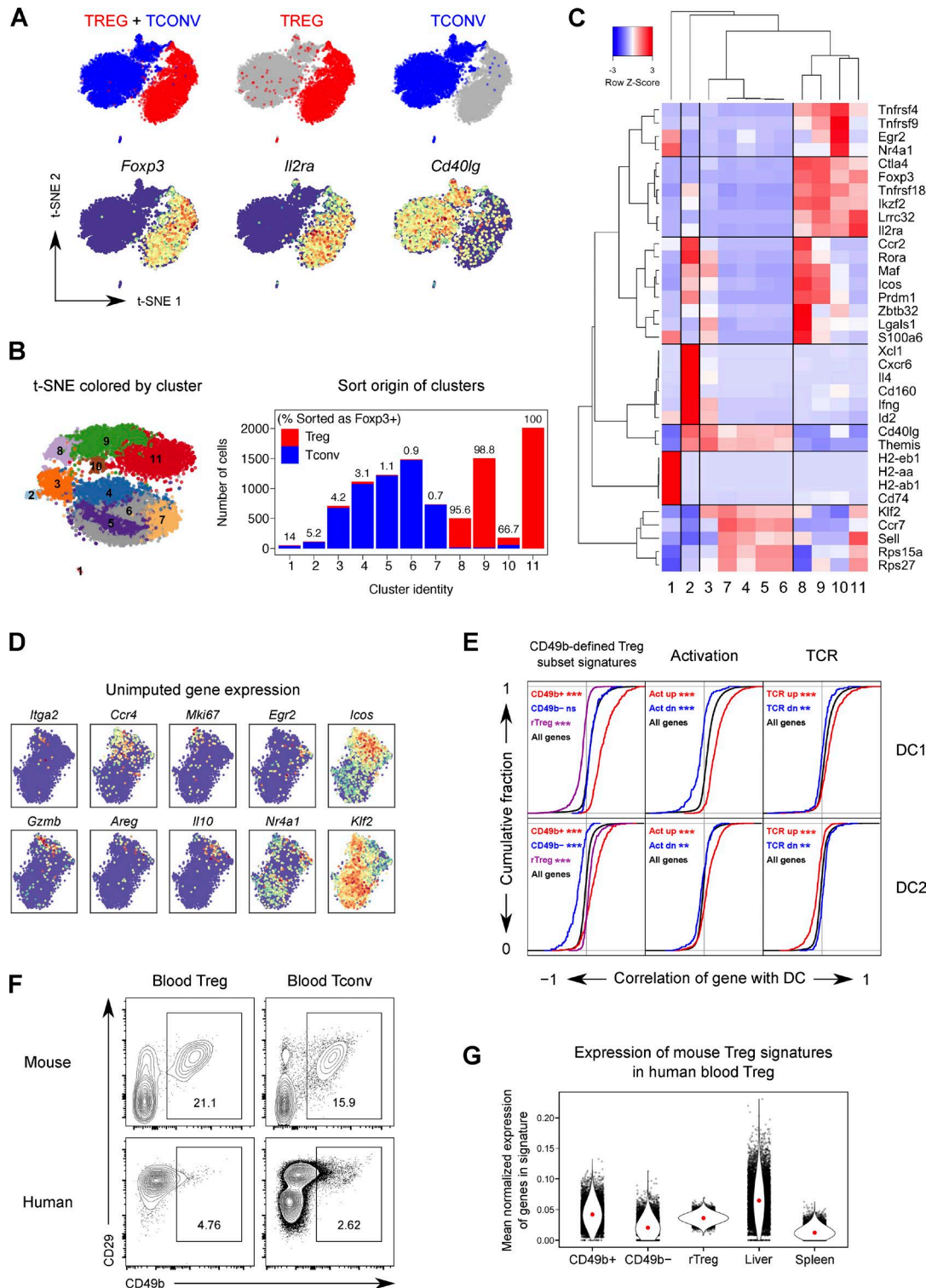


Figure S4. **Single-cell phenotypic landscape of splenic Treg and Tconv cells.** Related to Fig. 5. **(A)** t-SNE plot of scRNA-seq data of splenic Tconv and Treg cells, using simple histogram cutoffs for cell filtering instead of multivariate outlier detection. Cells colored red were sorted as Treg cells; blue cells were sorted as Tconv cells. **(B)** Left, t-SNE plot of combined splenic Tconv and Treg samples, filtered using multivariate outlier detection, colored by PhenoGraph clusters ( $k = 40$ ). Right, absolute number of cells in each PhenoGraph cluster, colored by sort origin. The percent sorted as *Foxp3*<sup>+</sup> is shown above each bar. **(C)** Mean expression of selected genes for each of the clusters from B. **(D)** t-SNE plot of Treg cells only, colored by the unimputed expression of selected genes. **(E)** Cumulative distribution of gene correlations with DC1 and DC2. The cumulative distribution of correlations for the bulk RNA-seq signatures of CD49b-defined Treg cell subsets, Treg cell activation, and Treg cell TCR-dependent gene expression are also shown. \*\*\*,  $p_{adj} \leq 10^{-10}$ ; \*\*,  $p_{adj} \leq 10^{-5}$ . **(F)** Representative staining of CD29 versus CD49b on CD4<sup>+</sup> *Foxp3*<sup>-</sup> Tconv and *Foxp3*<sup>+</sup> Treg cells from mouse or human blood. **(G)** Mean normalized expression of genes in each signature in human blood Treg cells. Each dot is a cell. Red dot, median.  $P < 10^{-10}$  by paired *t* test for comparisons between CD49b<sup>+</sup>/CD49b<sup>-</sup>/rTreg signatures, or between liver and spleen Treg signatures.

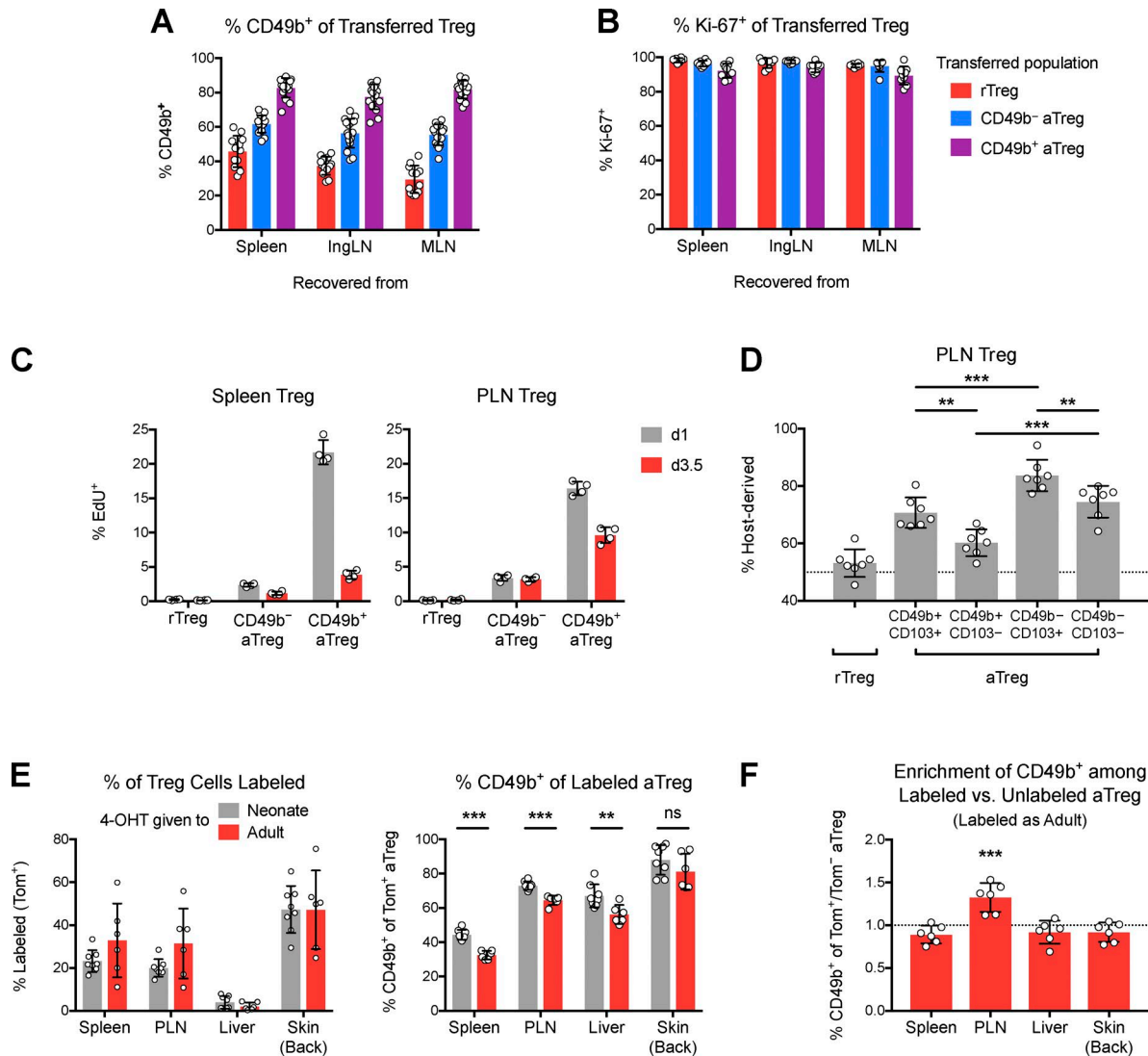


Figure S5. **Dynamics of CD49b<sup>+</sup> Treg cells.** Related to Fig. 4 and Fig. 6. **(A and B)** DT was administered to *Foxp3*<sup>GFP-DTR</sup> on days 0 and 1, and the indicated Treg subsets were separately transferred into mice 6 d after the second DT administration. Shown is the expression of CD49b (A) and Ki-67 (B) by transferred Treg cells 6 d after transfer. No differences in Tconv activation, proliferation, cell number, or cytokine production were observed (data not shown). Data were pooled from four (A) or two (B) independent experiments. **(C)** Percentage of Edu<sup>+</sup> cells among Treg subsets from spleen or PLNs 1 or 3.5 d after intravenous administration of Edu. **(D)** Chimerism of PLN Treg subsets after 12 d of parabiosis between congenic WT mice. Each point represents the average host chimerism of an independent pair of mice. Data are pooled from two independent experiments. **(E)** Left, labeling of Treg cells in various tissues 6 wk after 4-OHT was administered to 7-d-old neonatal or 6-wk-old adult *Foxp3*<sup>GFP-DTR</sup> *Cd4*<sup>ERT2-Cre</sup> *Rosa26*<sup>LSL-tdTomato</sup> mice. Right, percentage of CD49b<sup>+</sup> cells among fate-mapped (Tom<sup>+</sup>, tdTomato<sup>+</sup>) aTreg cells when 4-OHT was given to neonatal or adult mice. **(F)** Ratio of CD49b<sup>+</sup> frequency on tagged (Tom<sup>+</sup>) versus untagged (Tom<sup>-</sup>) aTreg cells 6 wk after 6-wk-old adult mice were given 4-OHT.

## References

- Arvey, A., J. van der Veecken, R.M. Samstein, Y. Feng, J.A. Stamatoyannopoulos, and A.Y. Rudensky. 2014. Inflammation-induced repression of chromatin bound by the transcription factor Foxp3 in regulatory T cells. *Nat. Immunol.* 15:580–587. <https://doi.org/10.1038/ni.2868>
- Chinen, T., A.K. Kannan, A.G. Levine, X. Fan, U. Klein, Y. Zheng, G. Gasteiger, Y. Feng, J.D. Fontenot, and A.Y. Rudensky. 2016. An essential role for the IL-2 receptor in T<sub>reg</sub> cell function. *Nat. Immunol.* 17:1322–1333. <https://doi.org/10.1038/ni.3540>
- Levine, A.G., S. Hemmers, A.P. Baptista, M. Schizas, M.B. Faire, B. Moltedo, C. Konopacki, M. Schmidt-Supprian, R.N. Germain, P.M. Treuting, and A.Y. Rudensky. 2017. Suppression of lethal autoimmunity by regulatory T cells with a single TCR specificity. *J. Exp. Med.* 214:609–622. <https://doi.org/10.1084/jem.20161318>